Statistical Modeling and Analysis for Robust Synthesis of Nanostructures

Tirthankar DASGUPTA, Christopher MA, V. Roshan JOSEPH, Z. L. WANG, and C. F. Jeff WU

We systematically investigate the best process conditions that ensure synthesis of different types of one-dimensional cadmium selenide nanostructures with high yield and reproducibility. Through a designed experiment and rigorous statistical analysis of experimental data, models linking the probabilities of obtaining specific morphologies to the process variables are developed. A new iterative algorithm for fitting a multinomial generalized linear model is proposed and used. The optimum process conditions, which maximize the preceding probabilities and make the synthesis process robust (i.e., less sensitive) to variations in process variables around set values, are derived from the fitted models using Monte Carlo simulations.

Cadmium selenide has been found to exhibit one-dimensional morphologies of nanowires, nanobelts, and nanosaws, often with the three morphologies being intimately intermingled within the as-deposited material. A slight change in growth condition can result in a totally different morphology. To identify the optimal process conditions that maximize the yield of each type of nanostructure and, at the same time, make the synthesis process robust (i.e., less sensitive) to variations of process variables around set values, a large number of trials were conducted with varying process conditions. Here, the response is a vector whose elements correspond to the number of appearances of different types of nanostructures. The fitted statistical models would enable nanomanufacturers to identify the probability of transition from one nanostructure to another when changes, even tiny ones, are made in one or more process variables. Inferential methods associated with the modeling procedure help in judging the relative impact of the process variables and their interactions on the growth of different nanostructures. Owing to the presence of internal noise, that is, variation around the set value, each predictor variable is a random variable. Using Monte Carlo simulations, the mean and variance of transformed probabilities are expressed as functions of the set points of the predictor variables. The mean is then maximized to find the optimum nominal values of the process variables, with the constraint that the variance is under control.

KEY WORDS: Cadmium selenide nanostructures; Generalized linear model; Multinomial; Nanotechnology; Robust design; Statistical modeling.

1. INTRODUCTION

Nanotechnology is the construction and use of functional structures designed at the atomic or molecular scale with at least one characteristic dimension measured in nanometers (1 nm = 10^{-9} m, which is about 1/50,000 of the width of human hair). The size of these nanostructures allows them to exhibit novel and significantly improved physical, chemical, and biological properties, phenomena, and processes. Nanotechnology can provide unprecedented understanding of materials and devices and is likely to impact many fields. By using a nanoscale structure as a tunable physical variable, scientists can greatly expand the range of performance of existing chemicals and materials. Alignment of linear molecules in an ordered array on a substrate surface (self-assembled monolayers) can function as a new generation of chemical and biological sensors. Switching devices and functional units at the nanoscale can improve computer storage and operation capacity by a factor of a million. Entirely new biological sensors can facilitate early diagnostics and disease prevention of cancers. Nanostructured ceramics and metals have greatly improved mechanical properties, both in ductility and in strength.

Current research by nanoscientists typically focuses on novelty, discovering new growth phenomena and new morphologies. However, within the next 5 years there will likely be a shift in the nanotechnology community toward controlled and large-scale synthesis with high yield and reproducibility. This transition from laboratory-level synthesis to large-scale, controlled, and designed synthesis of nanostructures necessarily demands systematic investigation of the manufacturing conditions under which the desired nanostructures are synthesized *reproducibly*, in *large* quantity, and with *controlled* or isolated morphology. Application of statistical techniques can play a key role in achieving these objectives. This article reports on a systematic study on the growth of one-dimensional cadmium selenide (CdSe) nanostructures through statistical modeling and optimization of the experimental parameters required for synthesizing desired nanostructures. This work is based on the experimental data presented in this article and research published in Ma and Wang (2005). Some general statistical issues and research opportunities related to the synthesis of nanostructures are discussed in the concluding section.

Cadmium selenide has been investigated over the past decade for applications in optoelectronics (Hodes, Albu-Yaron, Decker, and Motisuke 1987), luminescent materials (Bawendi, Kortan, Steigerwald, and Brus 1989), lasing materials (Ma, Ding, Moore, Wang, and Wang 2004), and biomedical imaging. It is the most extensively studied quantum-dot material and is, therefore, regarded as the model system for investigating a wide range of nanoscale processes. CdSe is found to exhibit the one-dimensional morphologies of nanowires, nanobelts, and nanosaws (Ma and Wang 2005), often with the three morphologies being intimately intermingled within the as-deposited material. Images of these three nanostructures obtained using a scanning electron microscope are shown in Figure 1.

In this experiment, the response is a vector whose elements correspond to the number of appearances of different types of

Tirthankar Dasgupta is Professor, School of Industrial and Systems Engineering, Georgia Institute of Technology, Altanta, GA 30332. Christopher Ma is Professor, School of Materials Science and Engineering, Georgia Institute of Technology, Atlanta, GA 30332. V. Roshan Josep is Professor, School of Industrial and Systems Engineering, Georgia Institute of Technology, Altanta, GA 30332. Z. L. Wang is Professor, School of Materials Science and Engineering, Georgia Institute of Technology, Atlanta, GA 30332. C. F. Jeff Wu is Professor, School of Industrial and Systems Engineering, Georgia Institute of Technology, Altanta, GA 30332 (E-mail: *jeffwu@isye.gatech.edu*). We are thankful to the associate editor and the referees, whose comments helped us to improve the contents and presentation of the article. The research of VRJ was supported by National Science Foundation (NSF) grant DMI-0448774. The research of ZLW was supported by grants from NSF, DARPA, and NASA.

DOI10.1198/00

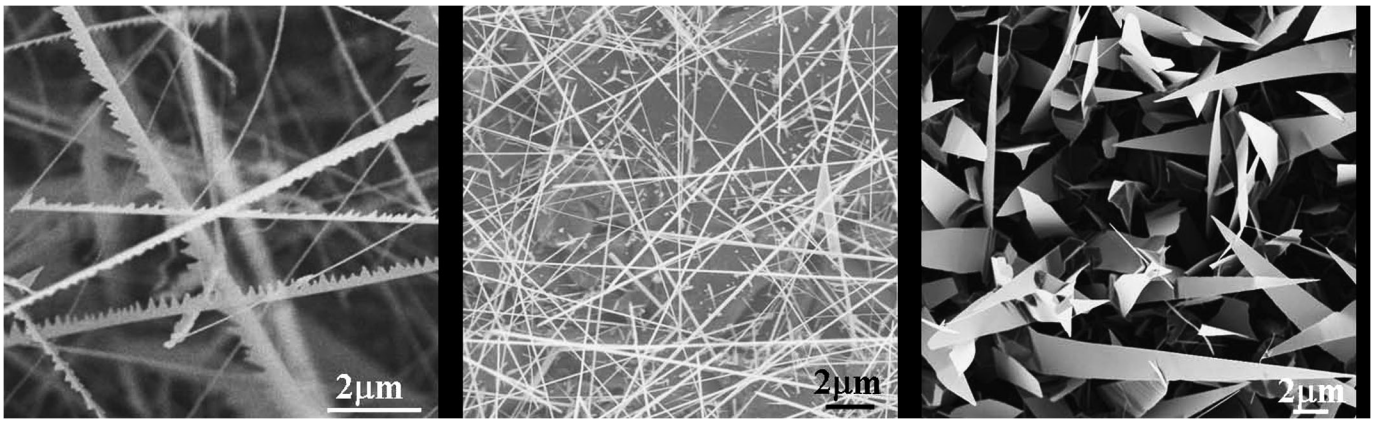

Figure 1. SEM images of nanostructures (from left to right: nanosaws, nanowires, nanobelts).

nanostructures and, hence, is a multinomial random variable. Thus, a multinomial generalized linear model (GLM) is the appropriate tool for analyzing the experimental data and expressing the multinomial logits as functions of the predictor variables (McCullagh and Nelder 1989; Faraway 2006). A new iterative algorithm for fitting a multinomial GLM that has certain advantages over the existing methods is proposed and implemented. The probability of obtaining each nanostructure is expressed as a function of the predictor variables. Owing to the presence of inner noise, that is, variation around the set value, each predictor variable is a random variable. Using Monte Carlo simulations, the expectation and variance of transformed probabilities are expressed as functions of the set points of the predictor variables. The expectation is then maximized to find the optimum set values of the process variables, ensuring at the same time that the variance is under control. The idea is, thus, similar to the two-step robust parameter design for larger-the-better responses (Wu and Hamada 2000, chap. 10).

This article is organized as follows. In Section 2 we give a brief account of the synthesis process, the experimental design, and the collection of data. Section 3 is devoted to fitting appropriate statistical models to the experimental data. This section consists of two subsections. In Section 3.1 a preliminary analysis using a binomial GLM is shown. Estimates of the parameters obtained here are used as initial estimates in the iterative algorithm for the multinomial GLM, which is developed and described in Section 3.2. In Section 4 we study the optimization of the process variables to maximize the expected yield of each nanostructure. Some general statistical issues and challenges in nanostructure synthesis and opportunities for future research are discussed in Section 5.

2. THE SYNTHESIS PROCESS, DESIGN OF EXPERIMENT, AND DATA COLLECTION

The CdSe nanostructures were synthesized (see Fig. 2) through a thermal evaporation process in a single-zone horizontal tube furnace (Thermolyne 79300). A 30-inch polycrystalline Al_2O_3 tube (99.9% purity) with an inner diameter of 1.5 inches was placed inside the furnace. Commercial-grade CdSe (Alfa Aesar, 99.995% purity, metal basis) was placed at the center of the tube as use as a source material. Single-crystal silicon substrates with a 2-nm thermally evaporated noncontinuous layer of gold were placed downstream of the source in order to collect the deposition of the CdSe nanostructures. The system was held at the set temperature and pressure for a period of 60 min and cooled to room temperature afterwards. The as-deposited products were characterized and analyzed by scanning electron microscopy (SEM; LEO 1530 FEG) or transmission electron microscopy (TEM; Hitachi HF-2000 FEG at 200 kV). As many as 180 individual nanostructures were counted from the deposition on each substrate.

The two key process variables affecting the morphology of CdSe nanostructures are temperature and pressure. A 5×9 full factorial experiment was conducted with five levels of source temperature (630, 700, 750, 800, 850°C) and nine levels of pressure (4, 100, 200, 300, 400, 500, 600, 700, 800 mbar). For a specific combination of source temperature and pressure, four to six substrates were placed downstream of the source to collect the deposition of nanostructures. The distance of the midpoint of the substrate from the source was measured and treated as a covariate.

Three experimental runs were conducted with each of the 45 combinations of temperature and pressure. However, these three runs cannot be considered to be replicates, because the number and location of substrates were not the same in the three runs. Consider, for example, the three runs performed with a temperature of 630°C and a pressure of 4 mbar. In the first run, six substrates were placed at distances of 1.9, 4.2, 4.9, 6.4, 8.1, and 10.2 cm from the source. In the second run, four substrates were placed at distances of 1.7, 4.6, 7.1, and 8.9 cm from the source. Seven substrates were placed at distances of 2.0, 4.3, 4.9, 6.4, 8.5, 10.6, and 13.0 cm from the source in

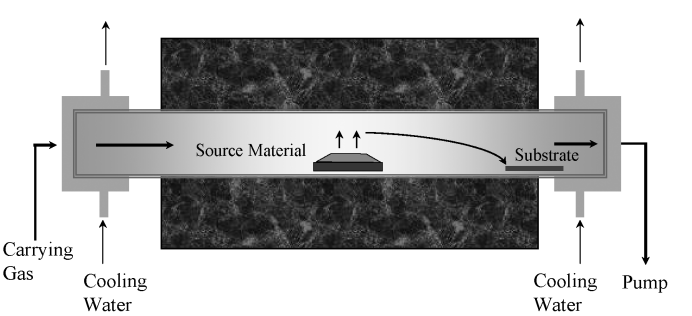

Figure 2. Synthesis process.

Table 1. Partial data (first 17 rows out of 415) obtained from the nanoexperiment

Temperature (°C)	Pressure (mbar)	Distance (cm)	Nanosaws	Nanowires	Nanobelts	No growth
630	4	12.4	0	0	0	180
630	4	14.7	74	106	0	0
630	4	15.4	59	121	0	0
630	4	16.9	92	38	50	0
630	4	18.6	0	99	81	0
630	4	20.7	0	180	0	0
630	4	12.2	50	94	36	0
630	4	15.1	90	90	0	0
630	4	17.6	41	81	58	0
630	4	19.4	0	121	59	0
630	4	12.5	49	86	45	0
630	4	14.8	108	72	0	0
630	4	15.4	180	0	0	0
630	4	16.9	140	40	0	0
630	4	19.0	77	47	56	0
630	4	21.1	0	88	92	0
630	4	23.5	0	0	0	180

the third run. Therefore, 17 ($= 6 + 4 + 7$) individual substrates were obtained with the temperature and pressure combination of (630°C, 4 mbar). Each of these 17 substrates constitutes a row in Table 1. The total number of substrates obtained from the 135 ($= 45 \times 3$) runs was 415. Note that this is not a multiple of 45 owing to an unequal number of substrates corresponding to each run.

By considering each of the 415 substrates as an experimental unit, the design matrix can, thus, be considered to be a 415×3 matrix, where the three columns correspond to source temperature (*TEMP*), pressure (*PRES*), and distance from the source (*DIST*). Each row corresponds to a substrate, on which a deposition is formed with a specific combination of *TEMP*, *PRES*, and *DIST* (see Table 1).

Recall that from the deposition on each substrate, 180 individual nanostructures were counted using SEM images. The response was, thus, a vector $\mathbf{Y} = (Y_1, Y_2, Y_3, Y_4)$, where Y_1, Y_2, Y_3, and Y_4 denote, respectively, the number of nanosaws, nanowires, nanobelts, and no morphology, with $\sum_{j=1}^{4} Y_j = 180$. For demonstration purposes, the first 17 rows of the complete dataset are shown in Table 1. These rows correspond to the temperature–pressure combination $(630, 4)$. The complete data can be downloaded from *www.isye.gatech.edu/~roshan*.

Almost no morphology was observed at a source temperature of 850°C. Therefore, results obtained from the 67 experimental units involving this level of temperature were excluded, and the data for the remaining 348 units were considered for analysis.

Henceforth, we shall use the suffixes 1, 2, 3, and 4 to represent quantities associated with nanosaws, nanowires, nanobelts, and no growth, respectively.

3. MODEL FITTING

3.1 Individual Modeling of the Probability of Obtaining Each Nanostructure Using Binomial GLM

Here, the response is considered binary, depending on whether we get a specific nanostructure or not. Let p_1, p_2, and p_3 denote, respectively, the probabilities of getting a nanosaw/nanocomb, nanowire, and nanobelt. Then, for $j = 1, 2, 3$, the marginal distribution of Y_j is binomial with $n = 180$ and probability of success p_j. The log-odds ratio of obtaining the jth type of morphology is given by

$$\zeta_j = \log \frac{p_j}{1 - p_j}.$$

Our objective is to fit a model that expresses the above log-odds ratios in terms of *TEMP*, *PRES*, and *DIST*.

From the main effects plot of *TEMP*, *PRES*, and *DIST* against observed proportions of nanosaws, nanowires, and nanobelts (Fig. 3), we observe that a quadratic model should be able to express the effect of each variable on p_j adequately. The interaction plots (not shown here) give a preliminary impression that all the three two-factor interactions are likely to be important. We, therefore, decide to fit a quadratic response model to the data.

Each of three process variables is scaled to $[-1, 1]$ by appropriate transformations. Let T, P, and D denote the scaled variables obtained by transforming *TEMP*, *PRES*, and *DIST*, respectively.

Using a binomial GLM with a logit link (McCullagh and Nelder 1989), we obtain the following models that express the log-odds ratios of getting a nanosaw/nanocomb, nanowire, and nanobelt as functions of T, P, and D:

$$\hat{\zeta}_1 = -.99 - .29T - 1.52P - 2.11D - .95T^2 - 1.30P^2 - 5.64D^2 - .18TP - 1.03PD + 4.29TD, \quad (1)$$

$$\hat{\zeta}_2 = -.56 + .82T - 2.53P - 1.59D - .58T^2 - 2.04P^2 - 2.62D^2 + 1.17TP - 1.44PD + .87DT, \quad (2)$$

$$\hat{\zeta}_3 = -1.68 + .19T - 1.88P - .58D - 1.69T^2 - .34P^2 - 3.20D^2 + .87TP - .94PD - 2.58TD. \quad (3)$$

All the terms are highly significant. The residual plots for all three models do not exhibit any unusual pattern.

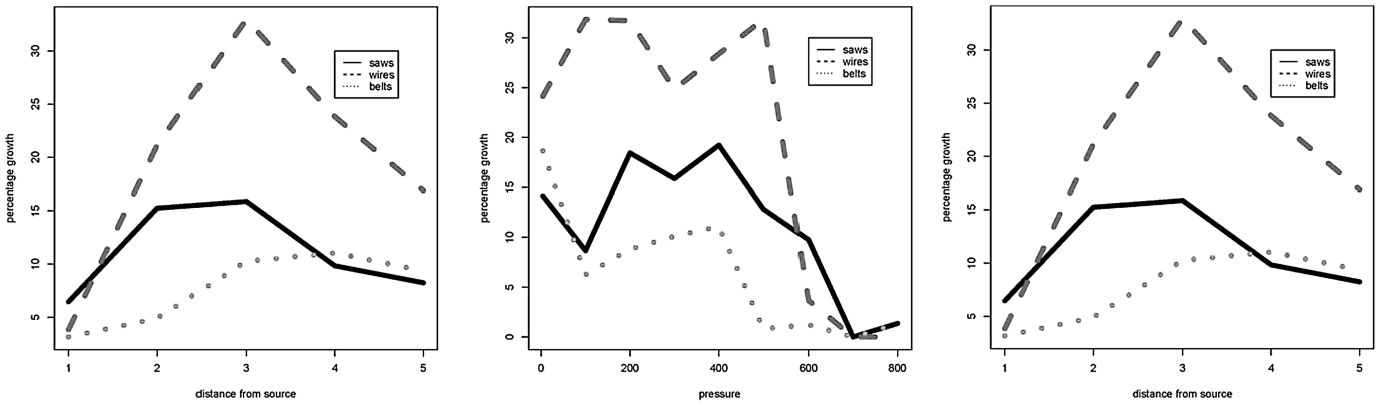

Figure 3. From left to right: growth versus temperature, growth versus pressure, growth versus distance.

3.2 Simultaneous Modeling of the Probability Vector Using Multinomial GLM

Denoting the probability of not obtaining any nanostructure by p_4, we must have $\sum_{j=1}^{4} p_j = 1$. Although the results obtained using the binomial GLM are easily interpretable and useful, the method suffers from the inherent drawback that, for specific values of T, P, and D, the fitted values of the probabilities may be such that $\sum_{j=1}^{3} p_j > 1$. This is due to the fact that the *correlation* structure of $\mathbf{Y}$ is completely ignored in this approach.

A more appropriate modeling strategy is to utilize the fact that the response vector $\mathbf{Y}$ follows a multinomial distribution with $n = 180$ and probability vector $\mathbf{p} = (p_1, p_2, p_3, p_4)$. In this case, one can express the multinomial logits $\eta_j = \log(\frac{p_j}{p_4})$, $j = 1, 2, 3$, as functions of T, P, and D. Note that η_j can be easily interpreted as the log-odds ratio of obtaining the jth morphology as compared to no nanostructure, with $\eta_4 = 0$.

Methods for fitting multinomial logistic models by maximizing the multinomial likelihood have been discussed by several authors (Aitkin, Anderson, Francis, and Hinde 1989; McCullagh and Nelder 1989; Agresti 2002; Faraway 2006; Long and Freese 2006). These methods have been implemented in several software packages such as R/S-plus (multinom function), STATA (.mlogit function), LIMDEP (Mlogit$ function), SAS (CATMOD function), and SPSS (Nomreg function). All of these functions use some algorithm for maximization of the multinomial likelihood (e.g., the multinom function in R/S-plus uses the neural network–based optimizer provided by Venables and Ripley 2002). They produce more or less similar outputs, the default output generally consisting of the model coefficients, their standard errors and z values, and model deviance.

Another popular algorithm to indirectly maximize the multinomial likelihood is to create a pseudo factor with a level for each data point and use a Poisson GLM with log link. This method, although appropriate for small datasets, becomes cumbersome when the number of data points is large. In the presence of a large number of levels of the pseudo factor, a large part of the output generated by standard statistical software such as R becomes redundant, because only the terms involving interaction between the categories and the predictor variables are of interest. Faraway (2006) pointed out some practical inconveniences of using this method. Its application to the current problem clearly becomes very cumbersome owing to the large number (348) of data points.

We propose a new iterative method of fitting multinomial logit models. The method is based on an iterative application of binomial GLMs. Besides the intuitive extension of binomial GLMs to a multinomial GLM, the method has certain advantages over the existing methods, which are described toward the end of this section.

Let $\mathbf{Y}_i = (Y_{i1}, \ldots, Y_{i4})$ denote the response vector corresponding to the ith data point, $i = 1$–N. Let $n_i = \sum_{j=1}^{4} Y_{ij}$. Here, $N = 348$ and $n_i = n = 180$ for all i. We have

$$P(Y_{i1} = y_{i1}, \ldots, Y_{i4} = y_{i4}) = \frac{n_i!}{y_{i1}! \cdots y_{i4}!} p_{i1}^{y_{i1}} \cdots p_{i4}^{y_{i4}}.$$

Thus, the likelihood function is given by

$$\begin{aligned} L(\mathbf{Y}_1, \ldots, \mathbf{Y}_N) &= \prod_{i=1}^{N} \frac{n_i!}{y_{i1}! \cdots y_{i4}!} p_{i1}^{y_{i1}} \cdots p_{i4}^{y_{i4}} \\ &= \prod_{i=1}^{N} \frac{n_i!}{y_{i1}! \cdots y_{i4}!} \prod_{j=1}^{3} \left(\frac{p_{ij}}{p_{i4}}\right)^{y_{ij}} p_{i4}^{\sum_{j=1}^{4} y_{ij}}. \end{aligned}$$

Defining $\eta_{ij} = \log \frac{p_{ij}}{p_{i4}}$, we have

$$p_{ij} = \frac{\eta_{ij}}{1 + \sum_{j=1}^{3} \exp(\eta_{ij})}, \qquad j = 1, 2, 3, \tag{4}$$

and

$$p_{i4} = \frac{1}{1 + \sum_{j=1}^{3} \exp(\eta_{ij})}. \tag{5}$$

Therefore, the log likelihood can be written as

$$\begin{aligned} &\log(L) \\ &= \sum_{i=1}^{N} \left(\log n_i! - \sum_{j=1}^{4} \log y_{ij}! + \sum_{j=1}^{3} y_{ij} \log \frac{p_{ij}}{p_{i4}} + n_i \log p_{i4} \right) \\ &= \sum_{i=1}^{N} \left(\log n_i! - \sum_{j=1}^{4} \log y_{ij}! + \sum_{j=1}^{3} y_{ij} \eta_{ij} \right. \\ &\qquad \left. - n_i \log \left(1 + \sum_{j=1}^{3} \exp(\eta_{ij}) \right) \right). \end{aligned} \tag{6}$$

Let $\mathbf{x}_i = (1, T_i, P_i, D_i, T_i^2, P_i^2, D_i^2, T_iP_i, P_iD_i, T_iD_i)'$, $i = 1, \ldots, N$. The objective is to express the η's as functions of $\mathbf{x}$. Substituting $\eta_{ij} = \mathbf{x}_i'\boldsymbol{\beta}_j$ in (6) and successively differentiating with respect to each $\boldsymbol{\beta}_j$, we get the maximum likelihood (ML) equations as

$$\sum_{i=1}^{N} \mathbf{x}_i \left(y_{ij} - n_i \frac{\exp(\eta_{ij})}{1 + \sum_{j=1}^{3} \exp(\eta_{ij})} \right) = \mathbf{0}, \qquad j = 1, 2, 3, \tag{7}$$

$$\sum_{i=1}^{N} \mathbf{x}_i \left(y_{14} - n_i \frac{1}{1 + \sum_{j=1}^{3} \exp(\eta_{ij})} \right) = \mathbf{0}, \tag{8}$$

where $\mathbf{0}$ denotes a vector of 0's having length 10. Writing $\exp(\gamma_{il}) = (1 + \sum_{l \neq j} \exp(\eta_{ij}))^{-1}$, we obtain from (7)

$$\sum_{i=1}^{N} \mathbf{x}_i \left(y_{ij} - n_i \frac{\exp(\eta_{ij} + \gamma_{ij})}{1 + \exp(\eta_{ij} + \gamma_{ij})} \right) = \mathbf{0}, \qquad j = 1, 2, 3. \tag{9}$$

Note that each equation in (9) is the ML equation of a binomial GLM with logit link. Thus, if some initial estimates of $\boldsymbol{\beta}_2, \boldsymbol{\beta}_3$ are available and, consequently, γ_{i1} can be computed, then $\boldsymbol{\beta}_1$ can be estimated by fitting a binomial GLM of Y_1 on $\mathbf{x}$. Similarly, $\boldsymbol{\beta}_2$ and $\boldsymbol{\beta}_3$ can be estimated. The following algorithm is, thus, proposed.

Binomial GLM-Based Iterative Algorithm for Fitting a Multinomial GLM. Let $\boldsymbol{\beta}_j^{(k)}$ be the estimate of $\boldsymbol{\beta}_j$, $j = 1, 2, 3$, at the end of the kth iteration.

Step 1. Using $\boldsymbol{\beta}_2^{(k)}$ and $\boldsymbol{\beta}_3^{(k)}$, compute $\eta_{i2}^{(k)} = \mathbf{x}_i'\boldsymbol{\beta}_2^{(k)}$ and $\eta_{i3}^{(k)} = \mathbf{x}_i'\boldsymbol{\beta}_3^{(k)}$ for $i = 1, \ldots, n$.

Step 2. Compute $\gamma_{i1}^{(k)} = \log \frac{1}{1+\exp(\eta_{i2}^{(k)})+\exp(\eta_{i3}^{(k)})}$, $i = 1, \ldots, n$.

Step 3. Treating Y_1 as the response and using the same design matrix, fit a binomial GLM with logit link. The vector of coefficients thus obtained is $\boldsymbol{\beta}_1^{(k+1)}$.

Step 4. Repeat Steps 1–3 by successively updating γ_{i2} and γ_{i3} and estimating $\boldsymbol{\beta}_2^{(k+1)}$ and $\boldsymbol{\beta}_3^{(k+1)}$.

Repeat Steps 1–4 until convergence. A proof of convergence is given in Appendix A. Note that we use the "offset" command in the statistical software R to separate the coefficients associated with η_1 from those with γ_1.

To obtain the initial estimates $\widehat{\eta}_{i2}^{(0)}$ and $\widehat{\eta}_{i3}^{(0)}$, we use the results obtained from the binomial GLM as described in Section 4.1. Let

$$\log \frac{\widehat{p}_{ij}}{1 - \widehat{p}_{ij}} = \mathbf{x}_i'\widehat{\boldsymbol{\delta}}_j, \tag{10}$$

where $\widehat{\boldsymbol{\delta}}_j$ is obtained using binomial GLM. Recalling the definition of η_{ij}, we get the initial estimates

$$\widehat{\eta}_{ij}^{(0)} = \log \frac{\widehat{p}_{ij}}{1 - \sum_{l=1}^{3} \widehat{p}_{il}}, \qquad j = 2, 3, \tag{11}$$

where $\widehat{p}_{il}$, $l = 1, 2, 3$, are estimated from (10). It is possible, however, that, for some i, $\sum_{l=1}^{3} \widehat{p}_{il} = \pi_i \geq 1$. For those data points, we provide a small correction as follows:

$$\widehat{p}_{il}^{c} = \begin{cases} \dfrac{\widehat{p}_{il}}{\pi_i}\left(1 - \dfrac{1}{2n_i}\right), & l = 1, 2, 3 \\ \dfrac{1}{2n_i}, & l = 4, \end{cases}$$

where $\widehat{p}_{il}^{c}$ denotes the corrected estimated probability. To justify the correction, we note that it is a common practice to give a correction of $\frac{1}{2n_i}$ (Cox 1970, chap. 3) in the estimation of probabilities from binary data. The correction given to category 4 is adjusted among the other three categories in the same proportion as the estimated probabilities. This ensures that $\widehat{p}_{il} > 0$ for all i and $\sum_{l=1}^{4} \widehat{p}_{il} = 1$.

In this example, there were 18 data points (out of 348) corresponding to which we had $\sum_{l=1}^{3} \widehat{p}_{il} \geq 1$. Following the procedure described previously to obtain the initial estimates, the following models were obtained after convergence:

$$\widehat{\eta}_1 = .42 - .12T - 3.08P - 3.68D - 1.84T^2 - 1.52P^2 - 9.09D^2 + .60TP - 2.31PD + 5.75TD, \tag{12}$$

$$\widehat{\eta}_2 = .54 + .88T - 3.85P - 3.13D - 1.21T^2 - 2.28P^2 - 5.26D^2 + 1.83TP - 2.62PD + 2.07TD, \tag{13}$$

$$\widehat{\eta}_3 = -.10 + .39T - 3.67P - 2.51D - 2.51T^2 - 1.12P^2 - 7.07D^2 + 1.72TP - 2.38PD + 4.47TD. \tag{14}$$

Inference for the Proposed Method. To test the significance of the terms in the model, one can use the asymptotic normality of the maximum likelihood estimates. Let $\mathbf{H}_\beta$ denote the 30×30 matrix consisting of the negative expectations of second-order partial derivatives of the log-likelihood function in (6), the derivatives being taken with respect to the components of $\boldsymbol{\beta}_1, \boldsymbol{\beta}_2$, and $\boldsymbol{\beta}_3$. By denoting the final estimator of $\boldsymbol{\beta}$ as $\boldsymbol{\beta}^*$, the estimated asymptotic variance–covariance matrix of the estimated model coefficients is given by $\boldsymbol{\Sigma}_{\beta^*} = \mathbf{H}_{\beta^*}^{-1}$. For a specific coefficient β_l, the null hypothesis $H_0 : \beta_l = 0$ can be tested using the test statistic $z = \widehat{\beta}_l / s(\widehat{\beta}_l)$, where $s^2(\widehat{\beta}_l)$ is the lth diagonal element of Σ_{β^*}.

Let $\beta_l^{(k)}$ denote the estimate of β_l obtained after the kth iteration of the proposed algorithm. Let $s^2(\beta_l^{(k)})$ denote the estimated asymptotic variance of $\beta_l^{(k)}$. It can easily be seen (App. B) that $s^2(\beta_l^{(k)})$ converges to $s^2(\beta_l^*)$. Thus, as the parameter estimates converge to the maximum likelihood estimates, their standard errors also converge to the standard error of the MLE. More generally, if $\boldsymbol{\Sigma}_{\beta^{(k)}}$ denotes the asymptotic covariance matrix of the parameter estimates at the end of the kth iteration, then $\boldsymbol{\Sigma}_{\beta^{(k)}} \to \boldsymbol{\Sigma}_{\beta^*}$.

The preceding property of the proposed algorithm ensures that one does not have to spend any extra computational effort in judging the significance of the model terms. The binomial GLM function in R used in every iteration automatically tests the significance of the model terms, and the p values associated with the estimated coefficients after convergence can be used for inference. Thus, the inferential procedures and diagnostic tools of the binomial GLM can easily be used in the multinomial GLM model. This is clearly an advantage of the proposed algorithm over existing methods. Further, the three models for nanosaws, nanobelts, and nanowires can be compared using

Table 2. Computed values of the test statistic for each estimated coefficient

	Nanosaws ($\widehat{\eta_1}$)			Nanowires ($\widehat{\eta_2}$)			Nanobelts ($\widehat{\eta_3}$)		
Term	$\hat{\beta}$	S.E.	p value	$\hat{\beta}$	S.E.	p value	$\hat{\beta}$	S.E.	p value
Intercept	.42	.24	.0807	.54	.25	.0343	−.10	.24	.6763
T	−.12	.30	.6855	.88	.28	.0020	.39	.38	.3125
P	−3.08	.41	.0000	−3.85	.50	.0000	−3.67	.51	.0000
D	−3.69	.67	.0000	−3.13	.57	.0000	−2.51	.66	.0001
T^2	−1.84	.34	.0000	−1.21	.27	.0000	−2.51	.34	.0000
P^2	−1.52	.44	.0006	−2.28	.52	.0000	−1.12	.54	.0381
D^2	−9.09	.99	.0000	−5.26	.66	.0000	−7.08	.77	.0000
TP	.60	.42	.1515	1.83	.41	.0000	1.72	.53	.0011
PD	−2.31	.83	.0053	−2.62	.70	.0000	−2.38	.84	.0043
TD	5.75	.80	.0000	2.07	.45	.0000	4.47	.69	.0000

these diagnostic tools. Such facilities are not available in the current implementation of other software packages.

In the fitted models given by (12)–(14), all 30 coefficients are seen to be highly significant with p values on the order of 10^{-6} or less. To check the model adequacy, we use the generalized R^2 statistic derived by Naglekerke (1991) defined as $R^2 = (1 - \exp((D - D_{\text{null}})/n))/(1 - \exp(-D_{\text{null}}/n))$, where D and D_{null} denote the residual deviance and the null deviance, respectively. The R^2 associated with the models for nanosaws, nanowires, and nanobelts are obtained as 61%, 50%, and 76%, respectively. This shows that the prediction error associated with the model for nanowires is the largest. This finding is consistent with the observation made by Ma and Wang (2005) that growth of nanowires is less restrictive compared to that of nanosaws and nanowires and can be carried out over wide ranges of temperature and pressure.

However, the small p values may also arise from the fact that some improper variance is used in testing. This overdispersion may be attributed to either some correlation among the outcomes from a given run in the experiment or some unexplained heterogeneity within a group owing to the effect of some unobserved variable. A multitude of external noise factors in the system make the second reason a more plausible one. We re-perform the testing by introducing three dispersion parameters σ_1^2, σ_2^2, and σ_3^2, which are estimated from the initial binomial fits using $\hat{\sigma}_j^2 = \chi_j^2/(N - 10)$, where χ_j^2 denotes Pearson's χ^2 statistic for the jth nanostructure, $j = 1, 2, 3$, and $N - 10 = 338$ is the residual degrees of freedom. The estimated standard errors of the coefficients and the corresponding p values are shown in Table 2.

From Table 2, we find that the linear effect of temperature is not significant for nanosaws and nanobelts. However, because the quadratic term T^2 and the interactions involving T are significant, we prefer to retain T in the models.

Note that although techniques for analyzing overdispersed binomial data are well known (e.g., Faraway 2006, chap. 2), methods for handling overdispersion in multinomial logit models are not readily available. The proposed algorithm provides us with a very simple heuristic way to do this and, thereby, has an additional advantage over the existing methods.

4. OPTIMIZATION OF THE SYNTHESIS PROCESS

In the previous sections, the three process variables have been treated as nonstochastic. However, in reality, none of these variables can be controlled precisely, and each of them exhibits certain fluctuations around the set (nominal) value. Such fluctuation is a form of noise, called *internal noise* (Wu and Hamada 2000, chap. 10), associated with the synthesis process and needs to be considered in performing optimization.

It is, therefore, reasonable to consider *TEMP*, *PRES*, and *DIST* as random variables. Let μ_{TEMP}, μ_{PRES}, and μ_{DIST} denote the set values of *TEMP*, *PRES*, and *DIST*, respectively. Then we assume

$$TEMP \sim \text{N}(\mu_{TEMP}, \sigma^2_{TEMP}),$$
$$PRES \sim \text{N}(\mu_{PRES}, \sigma^2_{PRES}),$$
$$DIST \sim \text{N}(\mu_{DIST}, \sigma^2_{DIST}),$$

where σ^2_{TEMP}, σ^2_{PRES}, and σ^2_{DIST} are the respective variances of *TEMP*, *PRES*, and *DIST* around their set values and are estimated from process data (Sect. 5.1). The task now is to determine the optimal nominal values of μ_{TEMP}, μ_{PRES}, and μ_{DIST} so that the expected yield of each nanostructure is maximized subject to the condition that the variance in yield is acceptable.

4.1 Measurement of Internal Noise in the Synthesis Process

Some surrogate process data collected from the furnace were used for estimation of the preceding variance components. Temperature and pressure were set at specific levels (those used in the experiment), and their actual values were measured repeatedly over a certain period of time. The range of temperature and pressure corresponding to each set value was noted. The variation in distance, which is due to repeatability and reproducibility errors associated with the measurement system, was assessed separately. The summarized data in Table 3 show the observed ranges of *TEMP*, *PRES*, and *DIST* against different nominal values. Under the assumption of normality, the range can be assumed to be approximately equal to six times the standard deviation.

We observe from Table 3 that, for the process variable *DIST*, the range of values around the nominal μ_{DIST} is constant ($2 \times .02 = .04$ mm) and independent of μ_{DIST}. Equating this range to $6\sigma_{DIST}$, we obtain an estimate of σ_{DIST} as $.04/6 = .067$ mm.

Similarly, for *TEMP*, the range can be taken to be almost a constant. Equating the mean range of 12.8 ($= 2 \times (2 \times 7 +$

Table 3. Fluctuation of process parameters around set values

Temperature (°C)		Pressure (mbar)		Distance (mm)	
Nominal value (μ_T)	Observed range ($\approx \pm 3\sigma_T$)	Nominal value (μ_P)	Observed range ($\approx \pm 3\sigma_P$)	Nominal value (μ_D)	Observed range ($\approx \pm 3\sigma_D$)
630	±7	4	±10	11	±.02
700	±7	100	±10	13	±.02
750	±6	200	±20	15	±.02
800	±6	300	±20	17	±.02
850	±6	400	±20	19	±.02
		500	±40	21	±.02
		600	±40		

$3 \times 6)/5)$°C to $6\sigma_{TEMP}$, an estimate of σ_{TEMP} is obtained as $12.8/6 = 2.13$°C.

The case of *PRES* is, however, different. The range, and hence σ_{PRES}, is an increasing function of μ_{PRES}. Corresponding to each value of μ_{PRES}, an estimate of σ_{PRES} is obtained by dividing the range by 6. Using these values of σ_{PRES}, the following regression line is fitted through the origin to express the relationship between σ_{PRES} and μ_{PRES}:

$$\sigma_{PRES} = .025\mu_{PRES}. \tag{15}$$

Recall that all the models are fitted with the transformed variables T, P, and D. The means μ_T, μ_P, and μ_D and the variances σ_T^2, σ_p^2, and σ_D^2 can easily be expressed in terms of the respective means and variances of the original variables.

4.2 Obtaining the Mean and Variance Functions of p_1, p_2, and p_3

From (4), we can write the estimated probability functions as $\widehat{p_j} = \exp(\widehat{\eta_j})/(1 + \sum_{j=1}^{3} \exp(\widehat{\eta_j}))$, where $\widehat{\eta_j}$ are given by (12)–(14).

Expressing $E(p_j)$ and $\mathrm{Var}(p_j)$ in terms of μ_T, μ_P, and μ_D is not a straightforward task. To do this, we use Monte Carlo simulations. For each of the 180 combinations of μ_{TEMP}, μ_{PRES}, and μ_{DIST} ($\mu_{TEMP} = 630$, 700, 750, and 800°C; $\mu_{PRES} = 4, 100, 200, \ldots, 800$ mbar; $\mu_{DIST} = 12$, 14, 16, 18, and 20 cm), the following are done:

1. μ_T, μ_P, and μ_D are obtained by appropriate transformation.
2. Five thousand observations on T, P, and D are generated from the respective normal distributions and η_j is obtained using (12), (13), or (14).
3. From the η_j values thus obtained, p_j's are computed using (4) and transformed to $\zeta_j = \log(p_j/(1 - p_j))$.
4. The mean and variance of those 5,000 ζ_j values [denoted by $\overline{\zeta_j}$ and $s^2(\zeta_j)$, respectively] are computed.
5. Using linear regression, $\bar{\zeta}_j$ and $\log s^2(\zeta_j)$ are expressed in terms of μ_T, μ_P, and μ_D.

4.3 Maximizing the Average Yield

Because the response here is of larger-the-better type, maximizing the mean is more important than minimizing the variance in the two-step optimization procedure (Wu and Hamada 2000, chap. 10) associated with robust parameter design.

The problem can thus be formulated as

$$\text{Maximize } \overline{\zeta_j} \text{ subject to } -1 \le \mu_T \le 1,\ -1 \le \mu_P \le 1,\ -1 \le \mu_D \le 1 \text{ for } j = 1, 2, 3.$$

Physically, this would mean maximizing the average log-odds ratio of getting a specific morphology.

The following models are obtained from the simulated data:

$$\begin{aligned}\overline{\zeta_1} = {} & -.75 + .20\mu_T - 1.02\mu_P - 1.39\mu_D - 1.50\mu_T^2 \\ & - 3.54\mu_P^2 - 11.02\mu_D^2 + 1.58\mu_T\mu_P \\ & - 2.22\mu_P\mu_D + 8.41\mu_T\mu_D, \end{aligned} \tag{16}$$

$$\begin{aligned}\overline{\zeta_2} = {} & -.40 + .80\mu_T - 2.96\mu_P - 1.43\mu_D - .98\mu_T^2 \\ & - 2.45\mu_P^2 - 6.05\mu_D^2 + 1.87\mu_T\mu_P \\ & - 3.41\mu_P\mu_D + 2.13\mu_T\mu_D, \end{aligned} \tag{17}$$

$$\begin{aligned}\overline{\zeta_3} = {} & -1.25 + .26\mu_T - 2.6\mu_P - .42\mu_D - 2.36\mu_T^2 \\ & - 1.24\mu_P^2 - 8.03\mu_D^2 + 1.74\mu_T\mu_P \\ & - 3.32\mu_P\mu_D + 4.57\mu_T\mu_D. \end{aligned} \tag{18}$$

Maximizing these three functions using the *optim* command in R, we get the optimal conditions for maximizing the expected yield of nanosaws, nanowires, and nanobelts in terms of μ_T, μ_P, and μ_D. These optimal values are transformed to the original units (i.e., in terms of μ_{TEMP}, μ_{PRES}, and μ_{DIST}) and are summarized in Table 4.

Contour plots of the average and variance of the yield probabilities of nanosaws, nanowires, and nanobelts against temperature and pressure (at optimal distances) are shown in Figure 4. The white regions on the top (average) panels and the black regions on the bottom (variance) panels are robust regions that promote high yield with minimal variation.

On the basis of these contour plots and the optimization output summarized in Table 4, the following conclusions can be drawn:

Table 4. Optimal process conditions for maximizing the expected yield of nanostructures

Nanostructure	Temperature (°C)	Pressure (mbar)	Distance (cm)
Nanosaws	630	307	15.1
Nanowires	695	113	19.0
Nanobelts	683	4	17.0

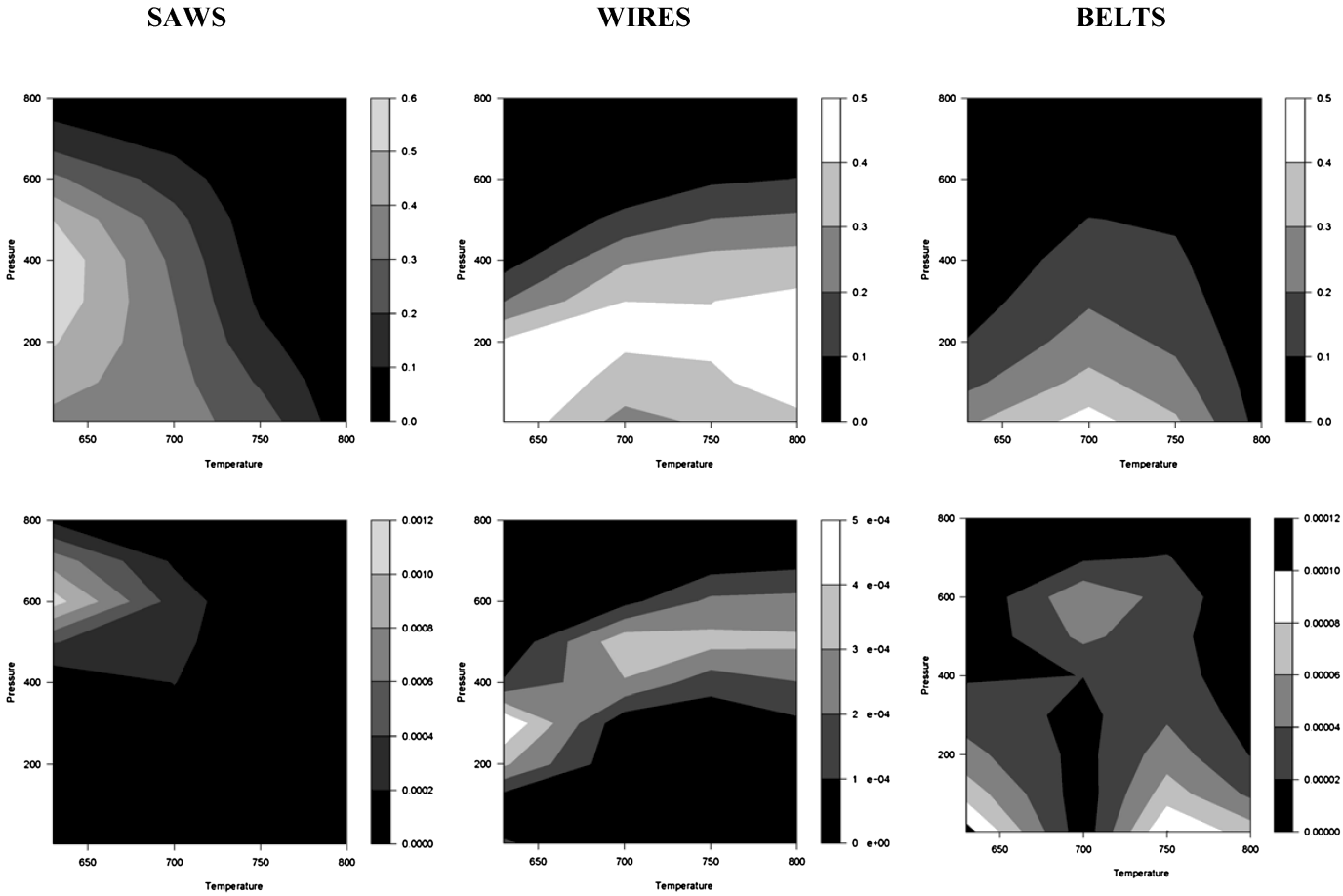

Figure 4. Contour plots.

1. For nanosaws, the process is fairly robust at a pressure below 400 mbar, irrespective of the source temperature.
2. For nanobelts, temperature affects robustness strongly, and for a pressure less than 400 mbar, the process is very robust only when the temperature is close to 700°C.
3. A temperature of around 630°C and a pressure of 310 mbar simultaneously maximize the average and minimize the variance of the probability of obtaining nanosaws.
4. A temperature of around 700°C and a pressure of around 120 mbar result in the highest average nanowire yield. Low variance is also observed in this region.
5. The highest nanobelt yield is achieved at a temperature of 680°C and a pressure of 4 mbar. This is also a low-variance region.
6. There is a large temperature–pressure region (white region in the top middle panel of Fig. 4) that promotes high and consistent nanowire yield.
7. The highest yields of nanobelts and nanowires are achieved at a higher distance (i.e., lower local temperature) as compared to nanosaws.

Except for the robustness-related conclusions, most of the preceding findings are summarized and discussed by Ma and Wang (2005). They also provide plausible and in-depth physical interpretations of some of these phenomena.

5. SOME GENERAL STATISTICAL ISSUES IN NANOMATERIAL SYNTHESIS AND SCOPE FOR FUTURE RESEARCH

In this article we report on an early application of statistical techniques in nanomaterial research. In terms of reporting results of experiments to synthesize nanostructures, this methodology can be considered a significant advancement over the rudimentary data analysis methods using simple graphs, charts, and summary statistics (e.g., Ma and Wang 2005; Song, Wang, Riedo, and Wang 2005) that have been reported in the nanomaterial literature so far. Here we discuss features of the data arising from a specific experiment and use a multinomial model to express the probabilities of three different morphologies as functions of the process variables. A new iterative algorithm, which is more appropriate than conventional methods for the present problem, is proposed for fitting the multinomial model. Inner noise is incorporated into the fitted models, and robust settings of process variables that maximize the expected yield of each type of nanostructure are determined.

Apart from the advantages discussed earlier in this article and mentioned by Ma and Wang (2005), this study demonstrates how statistical techniques can help in identifying important higher order effects (e.g., quadratic effects or complex interactions among the process variables) and how such knowledge can be used in fine-tuning the optimal synthesis conditions. This work is also an important step toward large-scale

controlled synthesis of CdSe nanostructures, because in addition to determining conditions for high yield, it also identifies robust settings of the process variables that are likely to guarantee consistent output.

Although statistical design of experiments (planning, analysis, and optimization) has been applied very successfully to various other branches of scientific and engineering research to determine high-yield and reproducible process conditions, its application in nanotechnology has been limited to date. Some unique aspects associated with the synthesis of nanostructures that make the application of the preceding techniques in this area challenging are (i) complete disappearance of nanostructure morphology with slight changes in process conditions; (ii) complex response surface with multiple optima, making exploration of optimal experimental settings very difficult (although in the current case study, a quadratic response surface was found more or less adequate, such is not the case in general); (iii) different types of nanostructures (saws, wires, belts) intermingled; (iv) categorical response variables in most cases; (v) functional inputs (control factors that are functions of time); (vi) a multitude of internal and external noise factors heavily affecting reproducibility of experimental results; and (vii) expensive and time-consuming experimentation. In view of these phenomena, the following are likely to be some of the major statistical challenges in the area of nanostructure synthesis:

1. *Developing a sequential space-filling design for maximization of yield*. Fractional factorial designs and orthogonal arrays are the most commonly used (Wu and Hamada 2000) designs, but are not suitable for nanomaterial synthesis, because the number of runs becomes prohibitively large as the number of levels increases. Moreover, they do not facilitate sequential experimentation, which is necessary to keep the run size to a minimum. Response surface methodology (Myers and Montgomery 2002) may not be useful because the underlying response surface encountered in nanoresearch can be very complex with multiple local optima, and the binary nature of data adds to the complexity. Space-filling designs such as Latin hypercube designs, uniform designs, and scrambled nets are highly suitable for exploring complex response surfaces with a minimum number of runs. They are now widely used in computer experimentation (Santner, Williams, and Notz 2003). However, they are used in the literature for only one-time experimentation. We need designs that are model independent, quickly "carve out" regions with no observable nanostructure morphology, allow for the exploration of complex response surfaces, and can be used for sequential experimentation.
2. *Developing experimental strategies where one or more of the control variables is a function of time*. In experiments for nanostructure synthesis, there are factors whose profiles or curves with respect to time are often crucial with respect to the output. For example, although the peak temperature is a critical factor, how this temperature is attained over time is very important. There is an ideal curve that is expected to result in the best performance. Planning and analysis of experiments with such factors (which are called *functional factors*) are not discussed much in the literature and may be an important topic for future research.
3. *Scale-up*. One of the important future tasks of the nanotechnology community is to develop industrial-scale manufacture of the nanoparticles and devices that are rapidly being developed. This transition from laboratory-level synthesis to large-scale, controlled, and designed synthesis of nanostructures poses plenty of challenges. The key issues to be addressed are rate of production, process capability, robustness, yield, efficiency, and cost. The following specific tasks may be necessary: (1) deriving specifications for key quality characteristics of nanostructures based on intended usage [quality loss functions (Joseph 2004) may be used for this purpose]; (2) expanding the laboratory setup to simulate additional conditions that are likely to be present in an industrial process; (3) conducting experiments and identifying robust settings of the process variables that will ensure manufacturing of nanostructures of specified quality with high yield; and (4) statistical analysis of experimental data to compute the capability of the production process with respect to each quality characteristic.

APPENDIX A: PROOF OF CONVERGENCE OF THE PROPOSED ALGORITHM

For simplicity, consider a single predictor variable and assume that $\eta_{ij} = \beta_j x_i$, where β_j is a scalar ($i = 1, 2, \ldots, N$, $j = 1, 2, 3$). Let $Q(\beta_1, \beta_2, \beta_3) = \sum_{i=1}^{N} (\sum_{j=1}^{3} y_{ij}\eta_{ij} - n_i \log(1 + \sum_{j=1}^{3} \exp(\eta_{ij})))$. Recall that $\beta_j^{(k)}$ denotes the estimate of β_j obtained after the kth iteration. Then it suffices to show that (i) $Q(\beta_1, \beta_2, \beta_3)$ is a concave function of β_j, $j = 1, 2, 3$, and (ii) $Q(\beta_1^{(k+1)}, \beta_2^{(k)}, \beta_3^{(k)}) \geq Q(\beta_1^{(k)}, \beta_2^{(k)}, \beta_3^{(k)})$.

It is easy to see that, for $l = 1, 2, 3$,

$$\frac{\partial^2 Q}{\partial \beta_l^2} = -\sum_{i=1}^{N} \frac{n_i x_i^2 e^{\beta_l x_i}(1 + \sum_{j \neq l} e^{\beta_j x_i})}{(1 + \sum_{j=1}^{3} e^{\beta_j x_i})^2} \leq 0,$$

which proves the concavity of Q.

To prove (ii), we note that, for given $\beta_2^{(k)}$, $\beta_3^{(k)}$, the solution for β_1 in the equation

$$\sum_{i=1}^{N} \left(y_{i1} - n_i \frac{e^{\beta_1 x_i}}{1 + e^{\beta_1 x_i} + \sum_{j=2}^{3} e^{\beta_j^{(k)} x_i}} \right) x_i = 0$$

maximizes $Q(\beta_1, \beta_2^{(k)}, \beta_3^{(k)})$.

From the first equation of (9) and Steps 1–3 of the algorithm, we have

$$\sum_{i=1}^{N} \left(y_{i1} - n_i \frac{e^{\beta_1^{(k+1)} x_i}}{1 + e^{\beta_1^{(k+1)} x_i} + \sum_{j=2}^{3} e^{\beta_j^{(k)} x_i}} \right) x_i = 0,$$

which means $\beta_1^{(k+1)} = \arg\max Q(\beta_1, \beta_2^{(k)}, \beta_3^{(k)})$. Therefore, (ii) holds.

APPENDIX B: PROOF OF CONVERGENCE OF THE ESTIMATED COVARIANCE MATRIX

Again, for simplicity, consider a single predictor variable and assume that $\eta_{ij} = \beta_j x_i$, where β_j is a scalar ($i = 1, 2, \ldots, N$, $j = 1, 2, 3$). Let $\beta_j^{(k)}$ denote the estimate of β_j obtained after Steps 1–3

of the kth iteration and let β_j^* denote the final estimate of β_j obtained by the proposed algorithm.

The estimated asymptotic variance of $\beta_1^{(k)}$, denoted by $s^2(\beta_1^{(k)})$, is given by the negative expectation of $\frac{\partial^2 \log L_{b1}}{\partial \beta_1^2}|_{\beta_1^{(k)},\beta_2^{(k-1)},\beta_3^{(k-1)}}$, where $\log L_{b1}$ denotes the binomial log-likelihood function of y_{i1}, $i = 1, \ldots, N$, that corresponds to the first of the three equations in (9) and is given by

$$\log L_{b1} = \sum_{i=1}^{N} \log \binom{n}{y_{i1}} + \sum_{i=1}^{N} y_{i1}(\eta_{i1} + \gamma_{i1}) - n_i \sum_{i=1}^{N} \log\bigl(1 + \exp(\eta_{i1} + \gamma_{i1})\bigr).$$

Now, $s^2(\beta_1^*)$, the estimated asymptotic variance of β_1^*, is given by the negative expectation of $\frac{\partial^2 \log L}{\partial \beta_1^2}|_{\beta_j=\beta_j^*, j=1,2,3}$, where $\log L$ is the multinomial likelihood given by (6).

It can easily be seen that

$$\frac{\partial^2 \log L_{b1}}{\partial \beta_1^2} = -\sum_{i=1}^{N} n_i x_i^2 \frac{1 + \exp(\eta_{i2}) + \exp(\eta_{i3})}{(1 + \exp(\eta_{i1}) + \exp(\eta_{i2}) + \exp(\eta_{i3}))^2} = \frac{\partial^2 \log L}{\partial \beta_1^2}.$$

By convergence of $\beta_j^{(k)}$ to β_j^* for $j = 1, 2, 3$, it follows that $s^2(\beta_1^{(k)}) \longrightarrow s^2(\beta_1^*)$.

Similarly, each component in the covariance matrix $\mathbf{\Sigma}_{\beta^{(k)}}$ can be proven to converge to each component of $\mathbf{\Sigma}_{\beta^*}$.

[Received June 2006. Revised February 2007.]

REFERENCES

Agresti, A. (2002), *Categorical Data Analysis*, New York: Wiley.

Aitkin, M., Anderson, D. A., Francis, B. J., and Hinde, J. P. (1989), *Statistical Modelling in GLIM*, Oxford, U.K.: Clarendon Press.

Bawendi, M. G., Kortan, A. R., Steigerwald, M. L., and Brus, L. E. (1989), "X–Ray Structural Characterization of Larger Cadmium Selenide (CdSe) Semiconductor Clusters," *Journal of Chemical Physics*, 91, 7282–7290.

Cox, D. R. (1970), *Analysis of Binary Data*, London: Chapman & Hall.

Faraway, J. J. (2006), *Extending the Linear Model With R: Generalized Linear, Mixed Effects and Nonparametric Regression Models*, Boca Raton, FL: Chapman & Hall/CRC Press.

Hodes, G., Albu-Yaron, A., Decker, F., and Motisuke, P. (1987), "Three-Dimensional Quantum-Size Effect in Chemically Deposited Cadmium Selenide Films," *Physics Review B*, 36, 4215–4221.

Joseph, V. R. (2004), "Quality Loss Functions for Nonnegative Variables and Their Applications," *Journal of Quality Technology*, 36, 129–138.

Long, J. S., and Freese, J. (2006), *Regression Models for Categorical Dependent Variables Using Stata*, College Station, TX: Stata Press.

Ma, C., and Wang, Z. L. (2005), "Roadmap for Controlled Synthesis of CdSe Nanowires, Nanobelts and Nanosaws," *Advanced Materials*, 17, 1–6.

Ma, C., Ding, Y., Moore, D. F., Wang, X., and Wang, Z. L. (2004), "Single-Crystal CdSe Nanosaws," *Journal of the American Chemical Society*, 126, 708–709.

McCullagh, P., and Nelder, J. (1989), *Generalized Linear Models*, London: Chapman & Hall.

Myers, H. M., and Montgomery, D. C. (2002), *Response Surface Methodology: Process and Product Optimization Using Designed Experiments*, New York: Wiley.

Naglekerke, N. (1991), "A Note on a General Definition of the Coefficient of Determination," *Biometrika*, 78, 691–692.

Santner, T. J., Williams, B. J., and Notz, W. I. (2003), *The Design and Analysis of Computer Experiments*, New York: Springer-Verlag.

Song, J., Wang, X., Riedo, E., and Wang, Z. L. (2005), "Systematic Study on Experimental Conditions for Large-Scale Growth of Aligned ZnO Nanowires on Nitrides," *Journal of Physical Chemistry B*, 109, 9869–9872.

Venables, W. N., and Ripley, B. D. (2002), *Modern Applied Statistics With S–PLUS*, New York: Springer-Verlag.

Wu, C. F. J., and Hamada, M. (2000), *Experiments: Planning, Analysis, and Parameter Design Optimization*, New York: Wiley.